

Photon-assisted entanglement and squeezing generation and decoherence suppression via a quadratic optomechanical coupling

Zhucheng Zhang and Xiaoguang Wang*

Zhejiang Institute of Modern Physics, Department of Physics, Zhejiang University, HangZhou 310027, China

(Dated: July 30, 2021)

Entanglement and quantum squeezing have wide applications in quantum technologies due to their non-classical characteristics. Here we study entanglement and quantum squeezing in an open spin-optomechanical system, in which a Rabi model (a spin coupled to the mechanical oscillator) is coupled to an ancillary cavity field via a quadratic optomechanical coupling. We find that their performances can be significantly modulated via the photon of the ancillary cavity, which comes from photon-dependent spin-oscillator coupling and detuning. Specifically, a fully switchable spin-oscillator entanglement can be achieved, meanwhile a strong mechanical squeezing is also realized. Moreover, we study the environment-induced decoherence and dissipation, and find that they can be mitigated by increasing the number of photons. This work provides an effective way to manipulate entanglement and quantum squeezing and to suppress decoherence in the cavity quantum electrodynamics with a quadratic optomechanics.

I. INTRODUCTION

Entanglement and quantum squeezing, as fascinating quantum effects, are important resources in quantum technologies, such as quantum information [1, 2], quantum computing [3], quantum metrology [4, 5], and so on. Entanglement characterizes the correlations between observables that cannot be understood with the local realistic theories [6], which arouses great attention of many researchers. For example, entanglement has been realized in experiments with microscopic systems including atoms [7–9], ions [10, 11] and photons [12, 13]. For macroscopic systems, entanglement between an optical field and a macroscopic vibrating mirror has been shown to be generated by radiation pressure [14–21]. Meanwhile, entanglement between different mechanical oscillators has also been studied in various optomechanical systems [22–27]. Quantum squeezing is instead potentially useful for surpassing the quantum noise limit [5]. Many researchers design various systems to realize quantum squeezing. For example, researchers have obtained strong quadrature squeezing in a transparent crystal with a $\chi^{(2)}$ or a $\chi^{(3)}$ nonlinear polarization [28, 29]. What's more, an optomechanical system, in its steady state, was shown can mimic a medium with $\chi^{(3)}$ nonlinearities [30, 31], which motivates researchers to design lots of optomechanical systems to generate quantum squeezing of optical and mechanical modes [32–37]. To realize entanglement and quantum squeezing in macroscopic system has always been the focus of research, and the optomechanical system is undoubtedly a promising research platform.

Cavity quantum electrodynamics (QED) aims to study the quantum behavior of atoms (ions) confined in a specific space interacting with light fields [38]. In order to observe more abundant physical phenomena, researchers

have been working to expand research platforms. For example, a strong coupling between mechanical oscillator and atom has been investigated in the cavity QED combined with a linear optomechanics [39]. Recently, a quadratic optomechanics was introduced into the cavity QED to study the superradiant quantum phase transition [40, 41], which was found that the realized quantum phase transition can be immune to the no-go theorem. Besides, a fully switchable phonon blockade was also realized in this type of system [42]. In the quadratic optomechanics, the phonon potential can be modulated by the photon through the quadratic optomechanical coupling [43–45], which makes it possible to use photon to manipulate the properties of system. Thus, an interesting question is whether one can use photon to manipulate the entanglement or the quantum squeezing in the cavity QED combined with a quadratic optomechanics.

In order to investigate the entanglement and the quantum squeezing in the cavity QED combined with a quadratic optomechanics, here we consider a hybrid quantum system, i.e., a Rabi model (a spin coupled to the mechanical oscillator) coupled to an ancillary cavity field via a quadratic optomechanical coupling. In this hybrid system, photon-assisted spin-oscillator entanglement and mechanical squeezing are realized. Specifically, through controlling the number of photons in the auxiliary cavity, a fully switchable spin-oscillator entanglement can be achieved, meanwhile a strong mechanical squeezing is also realized. Moreover, the effects of the environment-induced decoherence and dissipation on the system can be mitigated by increasing the number of photons.

We should point out that the entanglement in the cavity QED combined with the quadratic optomechanics was studied in Ref. [41], which is associated with a single-photon-induced quantum phase transition. But the entanglement realized in their scheme needs an extremely strong quadratic optomechanical coupling (about a quarter of mechanical frequency), which still exists an experimental challenge. However, in our paper, we study entanglement and quantum squeezing in the open quan-

* xgwang1208@zju.edu.cn

tum model, and the realized entanglement and quantum squeezing come from photon-dependent spin-oscillator coupling and detuning. What's more, with the same system, the parameters used in our scheme have more potential for experimental implementation. It is fundamental important to realize fully switchable entanglement and strong quantum squeezing in the open macro-system, which should have wide applications in the field of modern quantum technologies.

The paper is organized as follows: In Sec. II, we describe the hybrid quantum model and analyze its experimental feasibility. In Sec. III and in Sec. IV, we derive photon-assisted spin-oscillator entanglement and mechanical squeezing, respectively. In addition, the effects of the environment-induced decoherence and dissipation on the system are also considered. Finally, we summarize our main results in Sec. V.

II. MODEL AND HAMILTONIAN

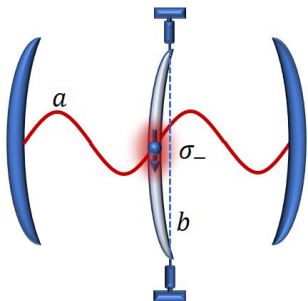


FIG. 1. Schematic diagram of the system. A two-level system σ_- (e.g., nitrogen-vacancy (NV) center spin) is coupled to a mechanical oscillator b . In addition, the mechanical oscillator is located in the node (or antinode) of the intracavity field a .

As shown in Fig. 1, we consider a hybrid optomechanical system, in which a mechanical oscillator is located in the node (or antinode) of the intracavity field, which can generate a quadratic optomechanical coupling [43–45]. Besides, a two-level system is coupled to the mechanical oscillator (e.g., a nitrogen-vacancy (NV) center spin embedded in diamond), which ultimately constitutes the Rabi model [46–48]. The total Hamiltonian of the system can be written as ($\hbar = 1$),

$$H = H_{an} + H_{rm} - ga^\dagger a (b^\dagger + b)^2, \quad (1)$$

with

$$H_{an} = \omega_a a^\dagger a, \quad (2)$$

$$H_{rm} = (\Omega/2)\sigma_z + \omega_b b^\dagger b + \lambda (b^\dagger + b) \sigma_x, \quad (3)$$

in which $a(a^\dagger)$ and $b(b^\dagger)$ denote the annihilation (creation) operators of the cavity (with resonant frequency ω_a) and mechanical (with resonant frequency ω_b) modes. g characterizes the quadratic optomechanical coupling.

H_{an} and H_{rm} describe the Hamiltonian of the cavity field and the Rabi model, respectively. σ_z and σ_x denote Pauli operators of the spin (with transition frequency Ω), and λ is the coupling strength between the spin and the oscillator.

From Eq. (1), one can find that the potential of oscillator is dependent on the intracavity photon number, so we can manipulate the properties of system via controlling the photon number. In other words, the cavity field a can be seen as an ancillary field, and in the following, we assume that the intracavity field a is prepared into the Fock state $|n\rangle$ ($n = 1, 2, 3, \dots$). Based on our scheme, the entanglement and the quantum squeezing are significantly manipulated by the photon as shown in the following sections. Through projecting the system Hamiltonian into the cavity field (Fock state) subspace, and then applying a squeezing transformation with squeezing operator $S(r_n) = \exp[r_n(b^2 - b^{\dagger 2})]$ (squeezing amplitude $r_n = -\frac{1}{4} \ln(1 - 4ng/\omega_b)$), Eq. (1) can be simplified as,

$$H_{eff} = S(r_n) H S^\dagger(r_n) = \frac{\Omega}{2} \sigma_z + \omega_n b^\dagger b + \lambda_n (b^\dagger + b) \sigma_x, \quad (4)$$

in which the constant term has been neglected, $\omega_n = \exp(-2r_n)\omega_b$ and $\lambda_n = \exp(r_n)\lambda$ are transformed mechanical frequency and spin-oscillator coupling strength, respectively.

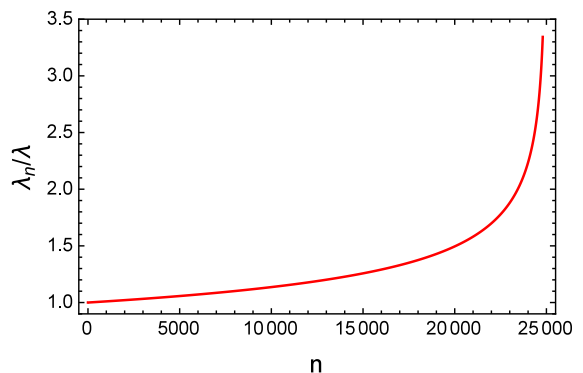


FIG. 2. Plot of the transformed spin-oscillator coupling strength λ_n as a function of the photon number n . The parameters are $\lambda = \kappa$ (κ is the decay rate of the oscillator), $\omega_b = 2000\kappa$ and $g = 10^{-5}\omega_b$.

As shown in Fig. 2, the transformed spin-oscillator coupling strength λ_n is plotted as a function of the photon number n . One can find that the transformed spin-oscillator coupling can be effectively enhanced with the increase of the photon. Here we should point out that, in our selected system parameters, the quadratic optomechanical coupling g is chosen to be $10^{-5}\omega_b$, which might be achieved in the optomechanical system by significantly enhancing the quadratic optomechanical coupling, and there are many theoretical and experimental schemes, such as near-field effects [49], fiber-cavity-based optomechanical device [50] and so on. Besides,

with the superconducting circuit [51], our scheme have more potential for experimental implementation than Ref. [41]. We should also point out that the enhancement of the spin-oscillator coupling dose not break the condition for the rotating wave approximation (RWA). Specifically, when the photon number $n = 20000$, the ratio $\omega_n/\lambda_n \approx 598$; when the photon number $n = 24000$, the ratio $\omega_n/\lambda_n \approx 179$. That is say, the RWA can still be adopted, and the effects caused by the anti-rotating wave term can be neglected. Thus, under the RWA, Eq. (4) in the interaction picture can be written as,

$$H_I = \lambda_n (b^\dagger \sigma_- e^{-i\Delta t} + b \sigma_+ e^{i\Delta t}), \quad (5)$$

in which $\Delta = \Omega - \omega_n$ is the photon-dependent detuning between the spin and the oscillator. One can find that the above Hamiltonian is actually a photon-dependent Jaynes-Cummings model.

III. PHOTON-ASSISTED SPIN-OSCILLATOR ENTANGLEMENT

In this section, we investigate the spin-oscillator entanglement. We consider that the initial state of the system is $|\psi(0)\rangle = |\uparrow, 0\rangle$, that is, the spin is in the spin-up state $|\uparrow\rangle$; and the oscillator is prepared into the ground state $|0\rangle$, which can be realized with the optical back action [52, 53]. One can find that with the interection Hamiltonian shown in Eq. (5), there is only the transition, i.e., $|\uparrow, 0\rangle \leftrightarrow |\downarrow, 1\rangle$. Thus, the system state at time t_1 can be assumed to be

$$|\psi(t_1)\rangle = c_{\uparrow,0}(t_1)|\uparrow, 0\rangle + c_{\downarrow,1}(t_1)|\downarrow, 1\rangle, \quad (6)$$

with the probability amplitudes $c_{\uparrow,0}(t_1)$ and $c_{\downarrow,1}(t_1)$. By substituting Eqs. (5)-(6) into the Schrödinger equation (see appendix for details), we can get the probability amplitudes as,

$$c_{\uparrow,0}(t_1) = \left[\cos\left(\frac{\tilde{\Omega}_n}{2}t_1\right) - i\frac{\Delta}{\tilde{\Omega}_n} \sin\left(\frac{\tilde{\Omega}_n}{2}t_1\right) \right] \exp(i\Delta t_1/2), \quad (7)$$

$$c_{\downarrow,1}(t_1) = -i\frac{\Omega_n}{\tilde{\Omega}_n} \sin\left(\frac{\tilde{\Omega}_n}{2}t_1\right) \exp(-i\Delta t_1/2), \quad (8)$$

in which $\Omega_n = 2\lambda_n$ can be seen as a photon-dependent quantum Rabi frequency, and $\tilde{\Omega}_n = \sqrt{\Omega_n^2 + \Delta^2}$ is rescaled quantum Rabi frequency due to the detuning Δ .

From the system state at t_1 , one can find that after the evolution, the oscillator and the spin evolve from a product state to an entangled state. The entangled state is a two-mode pure state, which can be measured by the concurrence [54]. Based on the definition of concurrence for pure state, we can get the concurrence at t_1 as

$$C = 2|c_{\uparrow,0}(t_1)c_{\downarrow,1}(t_1)|. \quad (9)$$

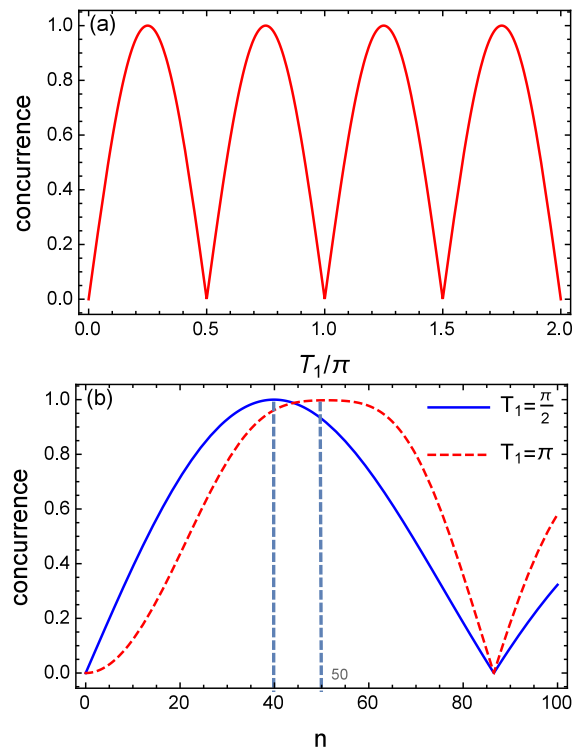


FIG. 3. The concurrence for the system state is plotted as a function of (a) the scaled time T_1 and (b) the photon number n , respectively. The parameters are (a) $n = 0$, $\Omega = \omega_b$, $T_1 = \kappa t_1$, (b) $T_1 = \pi/2, \pi$, and other parameters are the same as in Fig. 2.

As shown in Fig. 3, the concurrence of the system state is plotted as a function of the time and the photon number, respectively. From Fig. 3(a), one can observe that, when there are no photons in the ancillary cavity, the concurrence evolves with time periodically, and can reach to the maximum entanglement, i.e., the concurrence $C = 1$. In addition, at time $T_1 = \frac{\pi}{2}j$ ($j = 0, 1, 2, \dots$), the curve of concurrence is at the bottom of the valley, i.e., there is no entanglement between the spin and the oscillator. However, when we inject photons into the auxiliary cavity at these specific moments (e.g., $T_1 = \pi/2, \pi$), one can find from Fig. 3(b) that a fully switchable spin-oscillator entanglement can be achieved. In other words, through reasonably controlling the photon number in the auxiliary cavity, we can in principle achieve a high (without the appearance of the valley) entanglement degree between the spin and the oscillator in the evolution of time.

This manipulatable spin-oscillator entanglement comes from photon-dependent spin-oscillator coupling λ_n and detuning Δ , as shown in Eq. (5). Specifically, Due to that the spin-oscillator coupling and the dutuning can be adjusted by the photon number, the quantum Rabi frequency Ω_n is also dependent on the photon number, which results that the period of entanglement oscillation in evolution time can be manipulated. Hence, we can control the entanglement degree, as shown in Fig. 3(b).

We should point out that up to now, we have not considered the effects of environment-induced decoherence and dissipation on the system. In practice, these effects are not negligible factors. Now we investigate the environment-induced decoherence and dissipation after the entangled state $|\psi(t_1)\rangle$ has been prepared. We consider that the oscillator is in the thermal bath with thermal phonon number n_{th} , then the dynamics of system can be described by the following master equation,

$$\begin{aligned} \frac{d\rho}{dt} = & -i[H_I, \rho] + \frac{\kappa}{2}(n_{th} + 1)(2b\rho b^\dagger - b^\dagger b\rho - \rho b^\dagger b) \\ & + \frac{\kappa}{2}n_{th}(2b^\dagger \rho b - bb^\dagger \rho - \rho bb^\dagger) \\ & + \frac{\gamma_a}{2}(2\sigma_- \rho \sigma_+ - \sigma_+ \sigma_- \rho - \rho \sigma_+ \sigma_-), \end{aligned} \quad (10)$$

with the decay rates for oscillator (κ) and spin (γ_a).

When the environment-induced decoherence and dissipation are considered, the system state will no longer be a pure state. The density matrix $\rho(t)$ in the basis ($|1\rangle = |\uparrow, 0\rangle$, $|2\rangle = |\uparrow, 1\rangle$, $|3\rangle = |\downarrow, 0\rangle$, $|4\rangle = |\downarrow, 1\rangle$) can be written as

$$\begin{pmatrix} \rho_{11} & 0 & 0 & \rho_{14} \\ 0 & 0 & 0 & 0 \\ 0 & 0 & \rho_{33} & 0 \\ \rho_{41} & 0 & 0 & \rho_{44} \end{pmatrix}. \quad (11)$$

Substituting Eq. (11) into the master equation, one can get the time evolution of the matrix elements as follows,

$$\frac{d\rho_{11}}{dt} = -i\lambda_n(e^{i\Delta t}\rho_{41} - e^{-i\Delta t}\rho_{14}) - \gamma_a\rho_{11}, \quad (12)$$

$$\frac{d\rho_{14}}{dt} = -i\lambda_n e^{i\Delta t}(\rho_{44} - \rho_{11}) - \frac{\kappa(n_{th} + 1) + \gamma_a}{2}\rho_{14}, \quad (13)$$

$$\frac{d\rho_{33}}{dt} = \kappa(n_{th} + 1)\rho_{44} - \kappa n_{th}\rho_{33} + \gamma_a\rho_{11}, \quad (14)$$

$$\frac{d\rho_{41}}{dt} = i\lambda_n e^{-i\Delta t}(\rho_{44} - \rho_{11}) - \frac{\kappa(n_{th} + 1) + \gamma_a}{2}\rho_{41}, \quad (15)$$

$$\frac{d\rho_{44}}{dt} = i\lambda_n(e^{i\Delta t}\rho_{41} - e^{-i\Delta t}\rho_{14}) - \kappa(n_{th} + 1)\rho_{44} + \kappa n_{th}\rho_{33}. \quad (16)$$

The above differential equations can be solved numerically, then the density matrix $\rho(t)$ can be gotten.

From Eqs. (12)-(16), one can see that the density matrix of system will decay in the evolution with time due to the interaction between system and environment, in which the decay of diagonal moments corresponds to the loss of the system energy, while the decay of non-diagonal elements often accompanies the decay of quantum coherence [55]. Decoherence has always been a very important problem in quantum optics and quantum information. In order to investigate the role of photon of the auxiliary cavity in the interaction between system and environment, we numerically simulate the time evolution of diagonal and non-diagonal elements of the system density

matrix $\rho(t)$ under different photon numbers, respectively, as shown in Fig. 4.

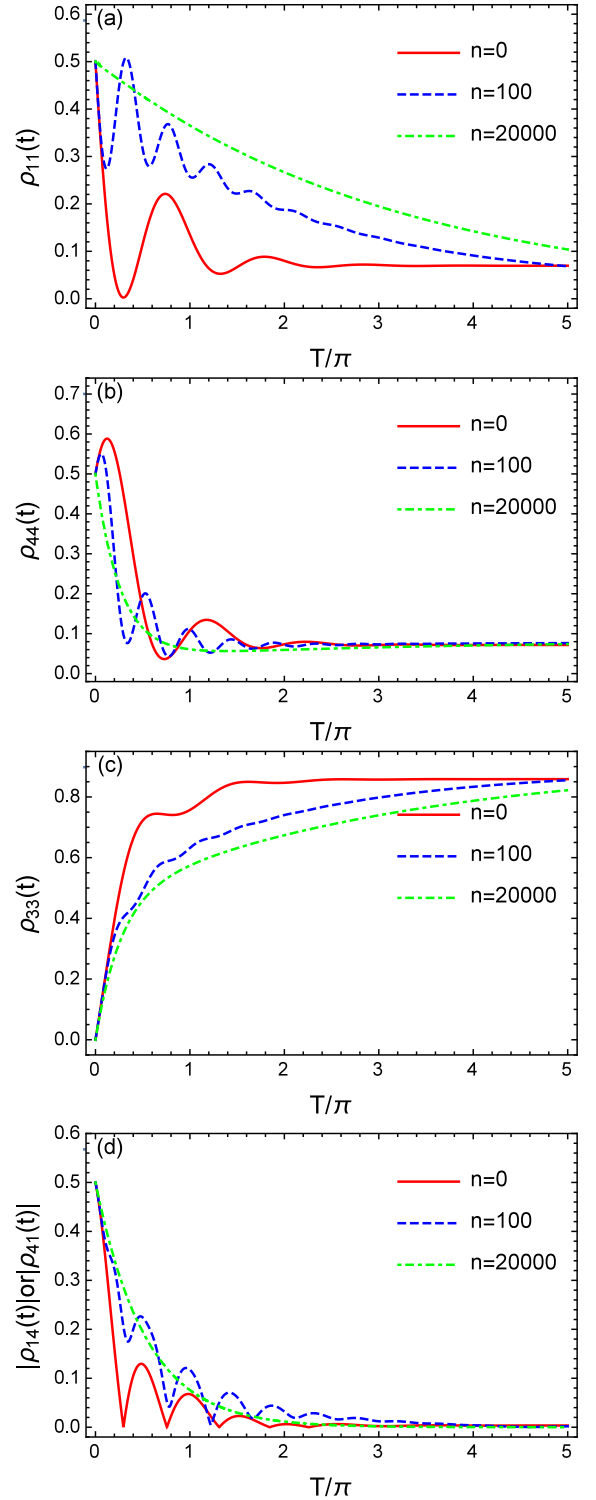


FIG. 4. The time evolution of diagonal and non-diagonal elements of the system density matrix $\rho(t)$ under different photon numbers. The scaled time $T = \kappa t$, $\gamma_a = 0.1\kappa$, $T_1 = 0.25\pi$, $n_{th} = 0.1$, and other parameters are the same as in Fig. 2.

From Fig. 4, under considering the interaction between the environment and the system, one can observe that the diagonal elements ρ_{11} and ρ_{44} evolve with time periodically, but their amplitudes gradually decrease. On the contrary, the amplitude of diagonal element ρ_{33} increases first and then keeps a certain value. This implies that the quantum state of system decays from the entangled state of $|\downarrow, 1\rangle$ and $|\uparrow, 0\rangle$ to the ground state $|\downarrow, 0\rangle$ gradually, accompanied by energy decaying from the system to the environment. Besides, the non-diagonal elements ρ_{14} and ρ_{41} also decays with time periodically, that is, the quantum coherence gradually disappears. However, one can also find that through increasing the photon number in the ancillary cavity, the transition from the entangled state to the ground state can be effectively mitigated (Fig. 4(c)), meanwhile, the decoherence can also be slowed down (Fig. 4(d)). Furthermore, when the number of photon is large enough, one can see that the curves of the time evolution will not oscillate anymore, which can be understood with the photon-dependent Rabi oscillation period t_r . The Rabi oscillation period t_r is inversely proportional to the Rabi oscillation frequency, i.e.,

$$t_r \sim \frac{1}{\Omega_n} \propto \frac{1}{n}. \quad (17)$$

Thus, the period of the oscillation will tend to zero if the number of photons is large enough, that is, the curves will evolve with time without oscillation. From the above analysis, we can see that with controlling the photon number in the ancillary cavity, the energy loss and the decoherence of the system can be effectively mitigated.

Now we investigate the effects of the photon on the spin-oscillator entanglement under the environment-induced dissipation and decoherence. Due to the dissipation and the decoherence, the system quantum state is a mixed state. Based on the definition of concurrence for the mixed state [54], we numerically simulate the time evolution of the concurrence with different photon numbers and thermal phonon numbers, as shown in Fig. 5. From the curves, one can observe that the concurrence evolves with time periodically, but its amplitude gradually decays to zero. This is because in the time evolution with dissipation and decoherence, the system quantum state gradually decays from the entangled state of $|\downarrow, 1\rangle$ and $|\uparrow, 0\rangle$ to the ground state $|\downarrow, 0\rangle$, meanwhile the system quantum coherence also decreases with time, which can be seen from Fig. 4. However, through increasing the photon number in the ancillary cavity, we can increase the time and the degree of the spin-oscillator entanglement. Besides, when the number of photon is large enough, one can also see that the curve of the concurrence will not oscillate anymore, which is due to the decrease of oscillation period t_r . Furthermore, from Fig. 5, one can find that, through increasing the photon number, the generated spin-oscillator entanglement is robust to the environment temperature.

From the above analysis, one can find that through manipulating the number of photon in the ancillary cav-

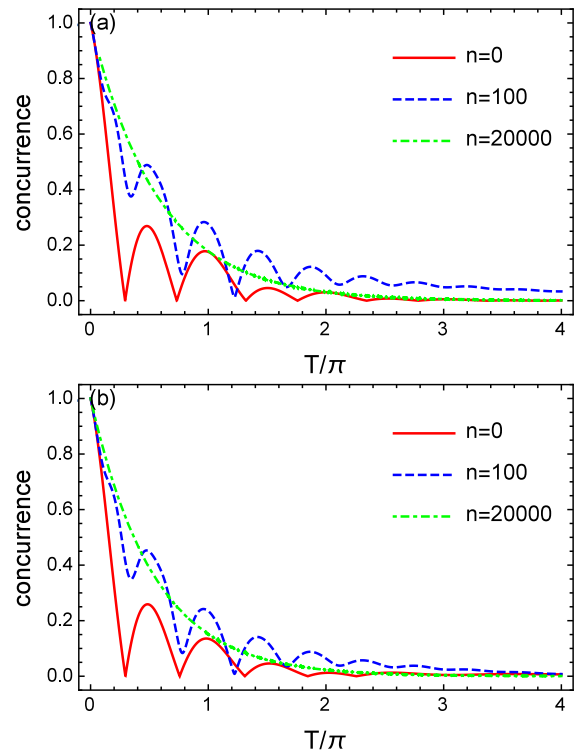


FIG. 5. The time evolution of the concurrence with different photon numbers and thermal phonon numbers under considering the environment-induced decoherence and dissipation. The parameters are: (a) $n_{th} = 0$, (b) $n_{th} = 0.1$, and other parameters are the same as in Fig. 4.

ity, a fully switchable spin-oscillator entanglement is realized, and under considering the environment-induced decoherence and dissipation, the time and the degree of entanglement can also be increased.

IV. PHOTON-ASSISTED MECHANICAL SQUEEZING

In this section, we investigate the situation where the detuning Δ between the spin and the oscillator is large enough, specifically, $\Delta \gg \lambda_n \sqrt{\langle b^\dagger b \rangle}$. Then, an effective Hamiltonian for the interaction Hamiltonian (i.e., Eq. (5)) can be derived as [56]

$$H'_{eff} = \chi [(b^\dagger b + 1) |\uparrow\rangle \langle \uparrow| - b^\dagger b |\downarrow\rangle \langle \downarrow|] \quad (18)$$

with $\chi = \frac{\lambda_n^2}{\Delta}$. Projecting the effective Hamiltonian H'_{eff} into the spin-up subspace, Eq. (18) becomes

$$\begin{aligned} H_\uparrow &= \langle \uparrow | H'_{eff} | \uparrow \rangle \\ &= \chi b^\dagger b, \end{aligned} \quad (19)$$

in which the constant term has been neglected.

From Eq. (19), one can see that, under the large detuning between the spin and the oscillator, the oscillator can

be decoupled with the spin, and is dependent on the photon of the ancillary cavity and the environment. Considering the dissipation induced by the oscillator-bath coupling, the quantum Langevin equation for the mechanical mode b can be derived as [57]

$$\dot{b} = -(\kappa + i\chi)b + \sqrt{2\kappa}b_{in}, \quad (20)$$

in which b_{in} is the noise operator for the thermal bath, and satisfies the following nonzero correlation functions,

$$\langle b_{in}^\dagger(t)b_{in}(t') \rangle = 2\pi n_{th}\delta(t-t'), \quad (21)$$

$$\langle b_{in}(t)b_{in}^\dagger(t') \rangle = 2\pi(n_{th} + 1)\delta(t-t'). \quad (22)$$

Besides, the noise operator b_{in} has a zero-mean value, that is, $\langle b_{in} \rangle = 0$.

Then, Eq. (20) can be solved analytically by the Laplace transform as follows [32, 37],

$$b(t) = f(t)b(0) + \sqrt{2\kappa} \int_0^t f(t-t')b_{in}(t')dt' \quad (23)$$

with

$$f(t) = \exp[-(\kappa + i\chi)t]. \quad (24)$$

Now we analyze the effects of the photon and the dissipation on the squeezing properties of the oscillator. The squeezing of the oscillator can be evaluated by the variances of its quadrature operators, $X_+ = S(r_n)(b^\dagger + b)S^\dagger(r_n)$ and $X_- = S(r_n)[i(b^\dagger - b)]S^\dagger(r_n)$, as follows [32, 37],

$$\begin{aligned} \langle \Delta X_\pm^2 \rangle(t) &= [1 + 2\langle b^\dagger b \rangle \pm (\langle b^2 \rangle + \langle b^{\dagger 2} \rangle)] \\ &\mp (\langle b^\dagger \rangle \pm \langle b \rangle)^2 e^{\pm 2r_n} \\ &= [1 + 2n_{th}(1 - e^{-2\kappa t})]e^{\pm 2r_n}, \end{aligned} \quad (25)$$

in which the oscillator is considered to be initially in the vacuum state, that is,

$$\langle b^\dagger(0)b(0) \rangle = 0. \quad (26)$$

From Eq. (25), one can find that the squeezing of the oscillator can only occur in $\langle \Delta X_-^2 \rangle(t)$, and there is a steady-state variance, i.e.,

$$\langle \Delta X_-^2 \rangle_{ss} = (1 + 2n_{th})e^{-2r_n}, \quad (27)$$

as shown in Fig. 6(a).

In order to further analyze the role of photon number in the generation of the mechanical squeezing, we also plot the steady-state variance $\langle \Delta X_-^2 \rangle_{ss}$ as a function of the photon number n for different thermal phonon numbers n_{th} , as shown in Fig. 6(b). One can obviously observe that the squeezing can be effectively manipulated by the photon. Specifically, when there are no photons in the ancillary cavity, there is no squeezing in the mechanical mode. However, through increasing the photon number, the mechanical squeezing occurs and the

squeezing degree can be optimized. For example, when the photon number $n = 24000$, the steady-state variance $\langle \Delta X_-^2 \rangle_{ss} \approx 0.2$. What's more, as long as the condition for the RWA is not broken, the mechanical mode can be further squeezed by continuously increasing the photon number, for example, when $n = 24800$, $\langle \Delta X_-^2 \rangle_{ss} \approx 0.09$. Besides, one can also find that the generated mechanical squeezing is robust to the environment temperature.

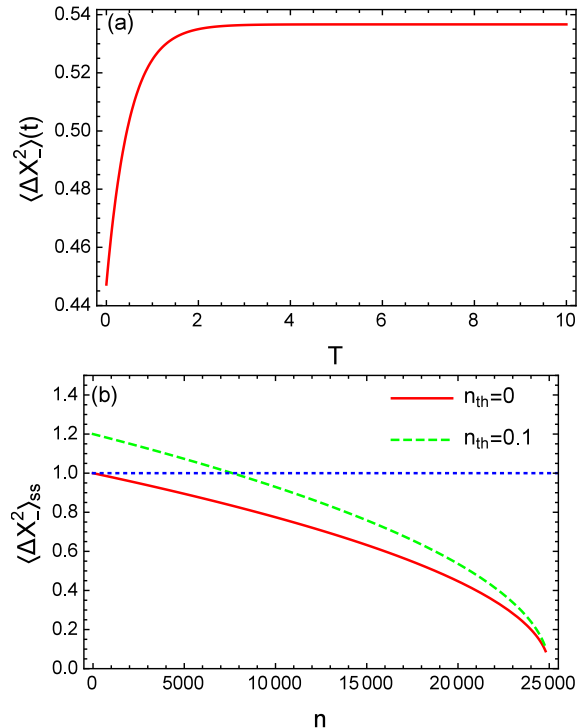


FIG. 6. (a) The time evolution of the time-dependent variance $\langle \Delta X_-^2 \rangle(t)$. (b) Plot of the steady-state variance $\langle \Delta X_-^2 \rangle_{ss}$ as a function of the photon number n for different thermal phonon numbers n_{th} , where above the dotted blue line, there is no squeezing in the mechanical mode, and below the line, there is squeezing. The parameters are: (a) $T = \kappa t$, $n = 20000$, $n_{th} = 0.1$; (b) $n_{th} = 0, 0.1$, and other parameters are the same as in Fig. 2.

V. CONCLUSION

In conclusion, we have studied spin-oscillator entanglement and mechanical squeezing in the open spin-optomechanical system. We showed that the spin-oscillator coupling and detuning can be effectively modulated by the photons of the ancillary cavity, which leads to the generation of a fully switchable spin-oscillator entanglement and a strong mechanical squeezing.

Besides, we also showed that under considering the environment-induced decoherence and dissipation, the entanglement time and degree between spin and oscillator can be significantly improved by increasing the number of photons, meanwhile a robust mechanical squeezing

can also be generated. This work realizes entanglement and quantum squeezing, and decoherence suppression in the open quantum system, which has potential applications in the quantum technologies.

ACKNOWLEDGMENT

This work was supported by the National Key Research and Development Program of China (Grants No. 2017YFA0304202 and No. 2017YFA0205700), the NSFC (Grants No. 11875231 and No. 11935012), and the Fundamental Research Funds for the Central Universities through Grant No. 2018FZA3005.

APPENDIX: SOLUTION OF THE SCHRÖDINGER EQUATION

By substituting Eqs. (5)-(6) into the Schrödinger equation, one can get the following differential equations on the probability amplitudes,

$$\frac{dc_{\uparrow,0}}{dt_1} = -i\frac{\Omega_n}{2}e^{i\Delta t_1}c_{\downarrow,1}, \quad (28)$$

$$\frac{dc_{\downarrow,1}}{dt_1} = -i\frac{\Omega_n}{2}e^{-i\Delta t_1}c_{\uparrow,0}, \quad (29)$$

with $\Omega_n = 2\lambda_n$.

In order to eliminate the time factors (i.e., $e^{-i\Delta t_1}$ and $e^{i\Delta t_1}$) in the above equations, one can replace them with the following new variables,

$$\tilde{c}_{\uparrow,0}(t_1) = c_{\uparrow,0}(t_1)e^{-i\frac{\Delta}{2}t_1}, \quad (30)$$

$$\tilde{c}_{\downarrow,1}(t_1) = c_{\downarrow,1}(t_1)e^{i\frac{\Delta}{2}t_1}. \quad (31)$$

Then we have following differential equations for the new variables,

$$\frac{d}{dt_1}\tilde{c}_{\uparrow,0} = -i\frac{\Delta}{2}\tilde{c}_{\uparrow,0} - i\frac{\Omega_n}{2}\tilde{c}_{\downarrow,1}, \quad (32)$$

$$\frac{d}{dt_1}\tilde{c}_{\downarrow,1} = -i\frac{\Omega_n}{2}\tilde{c}_{\uparrow,0} + i\frac{\Delta}{2}\tilde{c}_{\downarrow,1}. \quad (33)$$

These equations don't have time factors, which can be solved as,

$$\tilde{c}_{\uparrow,0}(t_1) = \cos\left(\frac{1}{2}\tilde{\Omega}_n t_1\right) - i\frac{\Delta}{\tilde{\Omega}_n}\sin\left(\frac{1}{2}\tilde{\Omega}_n t_1\right), \quad (34)$$

$$\tilde{c}_{\downarrow,1}(t_1) = -i\frac{\Omega_n}{\tilde{\Omega}_n}\sin\left(\frac{1}{2}\tilde{\Omega}_n t_1\right), \quad (35)$$

with $\tilde{\Omega}_n = \sqrt{\Omega_n^2 + \Delta^2}$. Thus, substituting the above results into Eqs. (30)-(31), one can get the solution of the Schrödinger equation.

-
- [1] S. L. Braunstein and P. V. Loock, *Rev. Mod. Phys.* **77**, 513 (2005).
- [2] R. Horodecki, P. Horodecki, M. Horodecki, and K. Horodecki, *Rev. Mod. Phys.* **81**, 865 (2009).
- [3] D. P. DiVincenzo, *Science* **270**, 255 (1995).
- [4] T. Eberle, S. Steinlechner, J. Bauchrowitz, V. Händchen, H. Vahlbruch, M. Mehmet, H. Müller-Ebhardt, and R. Schnabel, *Phys. Rev. Lett.* **104**, 251102 (2010).
- [5] V. B. Braginsky, V. B. Braginskii, and F. Y. Khalili, *Quantum measurement* (Cambridge University Press, 1995).
- [6] J. S. Bell, *Physics* (Long Island City, N.Y.) **1**, 195 (1964).
- [7] E. Hagley, X. Maitre, G. Nogues, C. Wunderlich, M. Brune, J. M. Raimond, and S. Haroche, *Phys. Rev. Lett.* **79**, 1 (1997).
- [8] B. Julsgaard, A. Kozhekin, and E. S. Polzik, *Nature* **413**, 400 (2001).
- [9] S. L. Su, X. Q. Shao, H. F. Wang, and S. Zhang, *Phys. Rev. A* **90**, 054302 (2014).
- [10] Q. A. Turchette, C. S. Wood, B. E. King, C. J. Myatt, D. Leibfried, W. M. Itano, C. Monroe, and D. J. Wineland, *Phys. Rev. Lett.* **81**, 3631 (1998).
- [11] D. Kielpinski, C. Monroe, and D. J. Wineland, *Nature* **417**, 709 (2002).
- [12] P. G. Kwiat, K. Mattle, H. Weinfurter, A. Zeilinger, A. V. Sergienko, and Y. Shih, *Phys. Rev. Lett.* **75**, 4337 (1995).
- [13] H. F. Wang and S. Zhang, *Phys. Rev. A* **79**, 042336 (2009).
- [14] D. Vitali, S. Gigan, A. Ferreira, H. R. Böhm, P. Tombesi, A. Guerreiro, V. Vedral, A. Zeilinger, and M. Aspelmeyer, *Phys. Rev. Lett.* **98**, 030405 (2007).
- [15] C. Genes, A. Mari, P. Tombesi, and D. Vitali, *Phys. Rev. A* **78**, 032316 (2008).
- [16] X. B. Yan, *Phys. Rev. A* **96**, 053831 (2017).
- [17] Z. J. Deng, X. B. Yan, Y. D. Wang, and C. W. Wu, *Phys. Rev. A* **93**, 033842 (2016).
- [18] Y. D. Wang, S. Chesi, and A. A. Clerk, *Phys. Rev. A* **91**, 013807 (2015).
- [19] S. Barzanjeh, D. Vitali, P. Tombesi, and G. J. Milburn, *Phys. Rev. A* **84**, 042342 (2011).
- [20] M. C. Kuzyk, S. J. van Enk, and H. Wang, *Phys. Rev. A* **88**, 062341 (2013).
- [21] C. G. Liao, R. X. Chen, H. Xie, and X. M. Lin, *Phys. Rev. A* **97**, 042314 (2018).
- [22] S. Huang and G. S. Agarwal, *New J. Phys.* **11**, 103044 (2009).
- [23] J. Q. Liao, Q. Q. Wu, and F. Nori, *Phys. Rev. A* **89**, 014302 (2014).
- [24] R. X. Chen, L. T. Shen, Z. B. Yang, H. Z. Wu, and S. B. Zheng, *Phys. Rev. A* **89**, 023843 (2014).
- [25] M. Wang, X. Y. Lü, Y. D. Wang, J. Q. You, and Y. Wu, *Phys. Rev. A* **94**, 053807 (2016).
- [26] J. Li, G. Li, S. Zippilli, D. Vitali, and T. Zhang, *Phys. Rev. A* **95**, 043819 (2017).
- [27] S. Chakraborty and A. K. Sarma, *Phys. Rev. A* **97**, 022336 (2018).

- [28] L. A. Wu, H. J. Kimble, J. L. Hall, and H. Wu, *Phys. Rev. Lett.* **57**, 2520 (1986).
- [29] L. Hilico, J. M. Courty, C. Fabre, E. Giacobino, I. Abram, and J. L. Oudar, *Appl. Phys. B* **55**, 202 (1992).
- [30] C. Fabre, M. Pinard, S. Bourzeix, A. Heidmann, E. Giacobino, and S. Reynaud, *Phys. Rev. A* **49**, 1337 (1994).
- [31] S. Mancini and P. Tombesi, *Phys. Rev. A* **49**, 4055 (1994).
- [32] E. A. Sete and H. Eleuch, *Phys. Rev. A* **82**, 043810 (2010).
- [33] F. Marino, F. S. Cataliotti, A. Farsi, M. S. de Cumis, and F. Marin, *Phys. Rev. Lett.* **104**, 073601 (2010).
- [34] D. W. C. Brooks, T. Botter, S. Schreppler, T. P. Purdy, N. Brahms, and D. M. Stamper-Kurn, *Nature* **488**, 476 (2012).
- [35] K. Jähne, C. Genes, K. Hammerer, M. Wallquist, E. S. Polzik, and P. Zoller, *Phys. Rev. A* **79**, 063819 (2009).
- [36] R. Almog, S. Zaitsev, O. Shtempluck, and E. Buks, *Phys. Rev. Lett.* **98**, 078103 (2007).
- [37] Z. C. Zhang, Y. P. Wang, Y. F. Yu, and Z. M. Zhang, *Opt. express* **26**, 11915 (2018).
- [38] H. Walther, B. T. H. Varcoe, B. G. Englert, and T. Becker, *Rep. Prog. Phys.* **69**, 1325 (2006).
- [39] K. Hammerer, M. Wallquist, C. Genes, M. Ludwig, F. Marquardt, P. Treutlein, P. Zoller, J. Ye, and H. J. Kimble, *Phys. Rev. Lett.* **103**, 063005 (2009).
- [40] X. Y. Lü, L. L. Zheng, G. L. Zhu, and Y. Wu, *Phys. Rev. Applied* **9**, 064006 (2018).
- [41] X. Y. Lü, G. L. Zhu, L. L. Zheng, and Y. Wu, *Phys. Rev. A* **97**, 033807 (2018).
- [42] L. L. Zheng, T. S. Yin, Q. Bin, X. Y. Lü, and Y. Wu, *Phys. Rev. A* **99**, 013804 (2019).
- [43] M. Bhattacharya, H. Uys, and P. Meystre, *Phys. Rev. A* **77**, 033819 (2008).
- [44] J. D. Thompson, B. M. Zwickl, A. M. Jayich, F. Marquardt, S. M. Girvin, and J. G. E. Harris, *Nature* **452**, 72 (2008).
- [45] J. C. Sankey, C. Yang, B. M. Zwickl, A. M. Jayich, and J. G. E. Harris, *Nat. Phys.* **6**, 707 (2010).
- [46] O. Arcizet, V. Jacques, A. Siria, P. Poncharal, P. Vincent, and S. Seidelin, *Nat. Phys.* **7**, 879 (2011).
- [47] S. D. Bennett, N. Y. Yao, J. Otterbach, P. Zoller, P. Rabl, and M. D. Lukin, *Phys. Rev. Lett.* **110**, 156402 (2013).
- [48] J. Teissier, A. Barfuss, P. Appel, E. Neu, and P. Maletinsky, *Phys. Rev. Lett.* **113**, 020503 (2014).
- [49] H. K. Li, Y. C. Liu, X. Yi, C. L. Zou, X. X. Ren, and Y. F. Xiao, *Phys. Rev. A* **85**, 053832 (2012).
- [50] N. E. Flowers-Jacobs, S. W. Hoch, J. C. Sankey, A. Kashkanova, A. M. Jayich, C. Deutsch, J. Reichel, and J. G. E. Harris, *Appl. Phys. Lett.* **101**, 221109 (2012).
- [51] E. J. Kim, J. R. Johansson, and F. Nori, *Phys. Rev. A* **91**, 033835 (2015).
- [52] M. Poggio, C. L. Degen, H. J. Mamin, and D. Rugar, *Phys. Rev. Lett.* **99**, 017201 (2007).
- [53] M. Bhattacharya and P. Meystre, *Phys. Rev. Lett.* **99**, 073601 (2007).
- [54] W. K. Wootters, *Phys. Rev. Lett.* **80**, 2245 (1998).
- [55] M. O. Scully and M. S. Zubairy, *Quantum optics* (Cambridge University Press, 1997).
- [56] C. Gerry, P. Knight, and P. L. Knight, *Introductory quantum optics* (Cambridge university press, 2005).
- [57] H. P. Breuer and F. Petruccione, *The theory of open quantum systems* (Oxford University Press, 2002).